International Journal of
INTELLIGENT SYSTEMS AND APPLICATIONS IN ENGINEERING
ISSN:2147-6799 www.ijisae.org Original Research Paper

Performance Improvement in ALGaN /GaN HEMT by High-K Approach

[1]Swati Dhondiram Jadhav, [2]Dr. Aboo Bakar Khan

Submitted: 16/07/2023 **Revised**: 07/09/2023 **Accepted**: 25/09/2023

Abstract: The integration of high-K dielectrics into AlGaN/GaN HEMTs opens up opportunities for future advancements in device design and fabrication In this work we have investigated the effect of field plate with the change in passivation layer using high-K technique. The materials are used are SiN, AL_2O_3, $HfSiO_4$, HfO_2, SiO_2 and observed the effects on electrical characteristic. The drain current is increased as the band gap of the material increases. After the simulation of proposed device, obtained drain current is 0.22A/mm with 31.81% improvement. It is also studies that threshold voltage is increased 3.4V. It is found that the threshold voltage percentage improvement is 25%. Further study includes that how gain depends on the dielectric material. Larger the value of dielectric constant larger the gain. By changing the passivation layer, gain of the device improved positively 121.13dB at 1MHz. It is shown that obtained Breakdown voltage is 300V for the material AL_2O_3 by considering all electrical parameters with field plate length of 0.4µm, 0.4µm Length of Gate and Dielectric (ε_r) value is 8.5 and it is completely depend on dielectric material. Tranconductance (Gm) is 0.15S/mm noticed and increased by 66.00 % positively. Additionally other electrical parameters are taken into the consideration such as cutoff Frequency is 76.0GHz at -2.1V with decrement of 9.63% and Capacitance between Gate and Source (C_{gsMax}) is 3.54×10^{-13}F/mm with 39.33 % improvement negatively, which has to take for tor future scope. The device is simulated by TCAD software.

***Keyword**: AlGaN/GaN HEMT, high-K dielectric, gate leakage current, performance improvement, power efficiency, threshold voltage.*

1. Introduction

High-K dielectric materials have emerged as promising solutions to address the limitations of traditional silicon dioxide (SiO_2) in advanced semiconductor devices. These materials possess a higher dielectric constant (K) than SiO_2, enabling improved gate control, reduced leakage current, and enhanced device performance. As a researcher embarks on writing a research paper focused on high-K techniques,

In this paper, we provide a comprehensive analysis of high-K techniques for writing research papers. This study delves into the fundamental concepts of high-K dielectrics, their properties, and the motivation behind their adoption in modern electronic devices. We will explore the challenges associated with traditional SiO_2-based gate dielectrics, such as the leakage current and electric-field scaling limit, which have necessitated the exploration of alternative high-K materials. This work discusses different high-k dielectric materials that have been extensively studied and employed in research and industry. These include metal oxides, such as hafnium oxide (HfO_2), zirconium oxide (ZrO_2), aluminum oxide (Al_2O_3), and rare earth oxides. In addition to material and integration considerations, this review addresses device performance metrics influenced by high-K techniques, such as threshold voltage (V_{TH}) modulation, sub threshold swing (SS), gate leakage current, and capacitance-voltage (C-V) characteristics. We discuss the impact of high-K dielectrics on these parameters and highlight their advantages and limitations.

This device is chosen due to the excellent characteristics such wide bandgap (3.4eV), high breakdown voltage, and large operation frequency. Bandgap of AlN is 6.2eV and a high breakdown field is 11 kV. By utilizing a self-aligned 20nm gate AlN/GaN HEMT offers the largest cutoff frequency 2.02 THz. It has been observed that, AlN/GaN HEMT gives two times higher value than AlGaN/GaN HEMT [1]–[9].

Similarly, 10nm T-gate lengths with high-K TiO_2 gate dielectric is taken into the consideration for enhancement-mode GaN metal-oxide-semiconductor high-electron-mobility transistor (MOS-HEMT) [10]. Additionally, For enhancement mode GaN MOS-HEMTs has offered

[1]Department of Electrical and Electronics Engineering Department.
Chatrapati Shivaji Maharaj University, Panvel, Maharashtra,
India.
swatijadhav5@gmail.com
[2]Department of Electrical and Electronics Engineering Department.
Chatrapati Shivaji Maharaj University, Panvel, Maharashtra,
India.
bakar3748@gmail.com

excellent version on account of a threshold voltage 1.07V, maximum extrinsic transconductance 1438mS/mm, saturation current at V_{GS}= 2V, 1A/mm, a maximum current is 2.55A/mm, unity-gain cut-off frequency is 524GHz, and with a record maximum oscillation frequency 758GHz.

In this [11]-[13] work the high-K Y_2O_3 through ultra-less permeability of oxygen, strength of high bonding, and more robustness of thermodynamic has been obtained. Correspondingly, the GaN MIS-HEMT has offered leakage of gate current as low as ~10-12 A/mm.

Moreover, the tiny effective thickness of oxide 2 nm to an ultralow SS 70 mV/dec, a maximum density of current is 600 mA/mm, gives excellent ability in control on gate. The appropriate aligned quality of semiconductor and dielectric has been invented to measure the capacitance versus voltage curve. Additionally, by adding two layers of dielectric, largest breakdown with high forward bias voltage and electric field is obtained such as 5.1V and 3.3MV/cm respectively. Similarly, the electric-field profiles between the gate and drain offers great electric-field with high-K method [14]. Certain Materials which has relative permittivity (ε_r) are taken into the consideration for GaN MIS-HEMTs as dielectric to the gate like Al_2O_3, HfO_2, ZrO_2 and TiO_2 with ε_r = 9, 20,30, and 55 respectively[15]-[18].

2. Device Geometry Structure

The proposed AlGaN/GaN HEMT using the high-K technique is shown in Figure. 1.

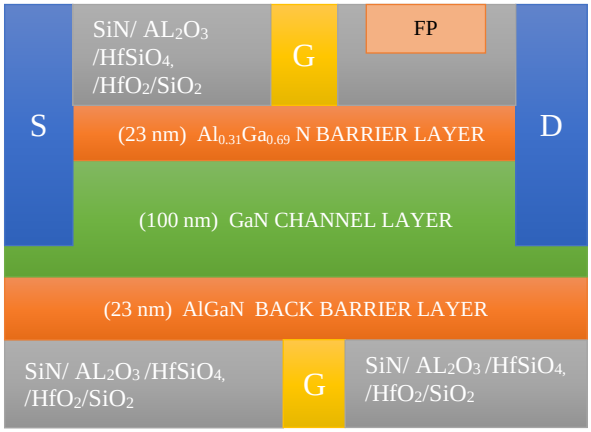

Fig 1. Proposed AlGaN/GaN HEMT using the high-K technique.

The mole fraction composition for both barriers was 31%. The performance of the proposed device can be classified into two categories: DC and AC performance.

To optimize the proposed device, the dimensions of the electrodes and layers are considered, as indicated in Table 1, for simulating the device in the Silvaco TCAD simulator.

Table 1. Proposed HEMT Device Geometry Dimensions

Parameters/Electrodes	Proposed HEMT Device Specifications
Length of Gate (L_G)	0.4 µm
Length of Field Plate (L_{FP})	0.4 µm
Distance Between Source-Gate (L_{GS})	1.1 µm
Distance Between Gate- Field Plate Length (L_{GFP})	0.4 µm
Length of Source (L_S)	0.1 µm
Length of Drain (L_D)	0.1 µm
AlGaN barrier and back barrier layer	23 nm
GaN channel	100 nm
Passivation Layer	0.1 µm

The formation of devices using various layers is described below. GaN channels have been utilized with different passivation materials, such as SiN /AL_2O_3 /$HfSiO_4$ /HfO_2 /SiO_2. The work function for the gate and source-drain electrodes was taken as 5eV with Schottky contact and 3.8eV with ohmic contacts, respectively. The material properties like band gap energy (E_g), Breakdown electric field (E_c), Relative dielectric constant (ε_r), Intrinsic carrier generation rate (n_i), Electron mobility (μ_n), Saturated drift velocity of electron (v_{sat}), Thermal conductivity (k) for SiN,AL_2O_3,$HfSiO_4$,HfO_2,SiO_2 are shown in Table 2.

2.1 Introduction to High-K

The working principle of high-electron-mobility transistors (HEMTs) is based on two-dimensional electron gas (2DEG). Researchers have worked on different techniques, such as Gate Engineering Techniques, Field Plate Techniques, Discrete Field Plate Techniques, and High-K, to improve the performance of HEMTs for high-power and high-frequency applications.

In the High-K Technique, a dielectric material acts as an insulator for the gate electrode. Modulating the electric field current flowing through the channel can be controlled. Permission to store a large amount of electric charge per unit of the gate is achieved using a high-K dielectric material.

2.2 Types of Materials in High-K

Several materials can be used as high-K dielectrics in high-electron-mobility transistors (HEMTs). Conventionally, Metal oxides, ferroelectric materials, III-V compounds, and organic materials are used as materials according to design requirements. In Concern with the Metal, oxides contain Aluminium oxide, Hafnium oxide (HfO_2), and Hafnium silicate ($HfSiO_4$) [19]-[24] are commonly used as high-K dielectric materials in HEMTs due to better thermal stability, high dielectric constants also a suitable candidate for use in high-power applications. The electrical characteristics were improved, such as an increase in the off-state breakdown voltage and reduction in the on-resistance, with the help of comparative studies with and without high-K dielectric materials used for high-power devices

[25]. Table 3 shows the electrical specifications with the simulated results for the drain current of the different high-K materials.

3. Model Discription

Mobility model, recombination model, carrier transport, and polarization models are analyzed for proposed device while simulating in Slivaco TCAD software [26].

$$P_{total} = [P_{PE\ (bottom)} + P_{SP(bottom)}] - [P_{PE(top)} + P_{SP(top)}]. \quad (1)$$

The P_{total} at the up/ down hetero interface relies on the material's polarization of spontaneous (P_{SP}) and piezoelectric (P_{PE}).

Shockley-Read-Hall (SRH) recombination model is used for fine transition in forbidden band gap because of states of trap. SRH recombination model is modeled in terms of lifetime of electrons, holes and trap energy level τ_n τ_p, and E_{trap} Also temperature respectively [27].

$$R_{net}^{SRH} = \frac{n - n_{ie}^2}{\tau_P\left[p + n_{ie}\exp\left(\frac{-E_{trap}}{KT}\right)\right] + \tau_n\left[p + n_{ie}\exp\left(\frac{-E_{trap}}{KT}\right)\right]} \quad (2)$$

The mobility model μ_0(T, N) can be written as follows [28]:

$$(T, N) = \mu_{\min}^{\beta_1}\left(\frac{T}{300}\right) + \frac{(\mu_{max} + \mu_{min})\left(\frac{T}{300}\right)^{\beta_2}}{1 + \left[\frac{N}{N_{ref}\left(\frac{T}{300}\right)^{\beta_3}}\right]^{\alpha\left(\frac{T}{300}\right)^{\beta_4}}} \quad (3)$$

Where, T denotes lattice temperature, N denotes total doping concentration, α is ionization rate.In specific to the ALBRECHT MODEL equation represents both mobility holes and electrons. Mobility models are ALBRECHT.N or ALBRECHT.P explained in following [29]:

$$\frac{1}{\mu_0(T, N)} = \frac{AN.ALBRCT.N}{NON.ALBRCT}\left(\frac{T_L}{TON.ALBRCT}\right)^{-3/2} \ln\left[1 + 3\left(\frac{T_L}{TON.ALBRCT}\right)^2 \times \left(\frac{T_L}{TON.ALBRCT}\right)^{-2/3}\right] + BN.ALBRCT \times \left(\frac{T_L}{TON.ALBRCT}\right)^{3/2} + \left[\frac{CN.ALBRCT}{\exp(TIN.ALBRCT/T_L) - 1}\right] \quad (4)$$

Newton method is used to achieve the best matching between the resultant equations for the proposed work which offers convergence in quadratic manner.

Material	SiN (Silicon Nitride)	$HfSiO_4$ (Hafnium Silicate)	HfO_2(Hafnium Oxide)	SiO_2 (Silicon Dioxide)	AL_2O_3 (Aluminum Oxide)
$E_g(eV)$	5.0	5.8	7	9.0	6.0
$E_c(MV/cm)$	1-10	3-6	6-10	10-20	15-20
$n_i(/cm^3)$	LOW	LOW	LOW	LOW	LOW
$\mathcal{E}_r$	6-8	14-22	20-25	3.9	8.5
$\mu_n(cm^2.V^{-1}.s^{-1})$	50-100	20-60	10-25	1000-1400	0.5-1.5
$v_{sat}(10^7\ cm/s)$	1.7	1.0	1.0	1.0	NA
k(W. $m^{-1}.K^{-1}$)	15-30	3-5	3-5	1.0-1.5	35-40

Table 2. Material properties for SiN, AL_2O_3, $HfSiO_4$, HfO_2, SiO_2.

4. Drain Current For Different Material AL_2O_3, HFO_2, SIO_2, $HFSIO_4$

Figure. 2 show AlGaN/GaN HEMT the geometry structure. For simulation, the Silvaco TCAD software is utilized by considering the electrical properties of different materials such as AL_2O_3, $HfSiO_4$, HfO_2, and SiO_2. The drain currents are compared. The results are shown in Figure 3. Initially passivation layer of material SiO_2 is kept for simulation of the device and also considered the all geometry dimension as mentioned in Table 1. The simulated drain current obtained is 0.206A/mm. Secondly; HfO_2 is taken into the consideration for the simulations, obtained drained current is noted 0.208 A/mm. In third step $HfSiO_4$ passivation layer is considered and at last AL_2O_3. The drain current for $HfSiO_4$ and AL_2O_3 are found as 0.214A/mm and 0.223 A/mm respectively. The drain current is increased as the band gap of the material increases.

Different-K Material ↓	Gap (eV)	Dielectric Constant (ε)	Darin Current (A/Mm)	Percentage Improvement w. r. t. Al_2O_3 (%)
AL_2O_3	8.8	~ 9	0.223	-
$HfSiO_4$	6.5	[5-6]	0.214	2.92
HfO_2	5.8	[2-5]	0.208	6.45
SiO_2	1.1	3.9	0.206	8.04
SiN	5.3	[7-8]	0.209	6

Table 3. Electrical Properties of Different Materials with Drain Current and Percentage Improvement.

AL_2O_3 similarly the drain currents for $HfSiO_4$, HfO_2, and SiO_2 are 0.214, 0.208, and 0.206A/mm, respectively. The percentage improvement of the drain current with respect to AL_2O_3 was also calculated and is shown in Table 1. It is obvious that we must consider a material that provides a larger drain current to optimize the device for high-frequency applications. Therefore for further work, we have considered the metal oxides contain aluminium oxide (AL_2O_3).

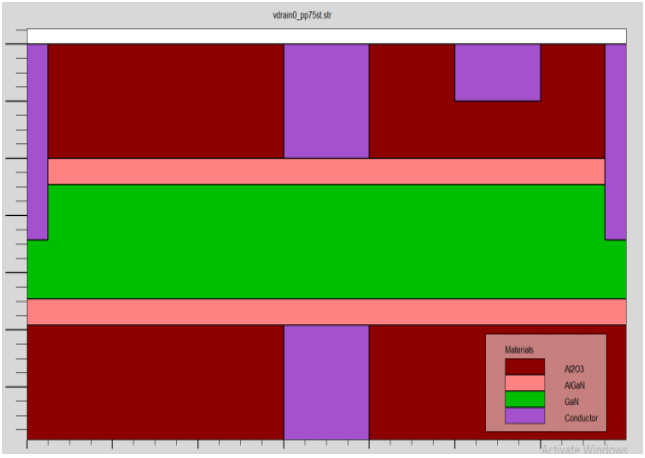

Fig 2. The proposed AlGaN/GaN HEMTs is a material AL_2O_3 Structure file.

4.1 Drain Current versus Gate voltage for different material high-K

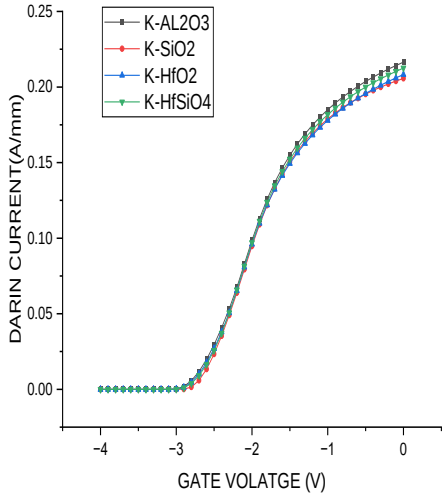

Fig 3. Drain Current versus Gate voltage for different material high-K.

5. Result Analyses For Proposed Hemt For The Material Al_2o_3

5.1. Drain Current versus Gate voltage

To analyse the device performance drain current is the vital parameter. Material with a high-K dielectric value controls the channel electric field, resulting in a drain current. The voltage current equation [30]:

$$I=I_S \times \exp\left[q(V_{GS} - R_S I_{GS}/\eta kT)\right] \quad (5)$$

Where I_S is the saturation current (I_S=SA*T^2exp(-qϕ_B/kT),

), S is contact area, A is plot of log (I_{GS} versus V_{GS} q is the electron charge, T is the temperature in kelvin η ideality factor, k is Boltzmann constant, R_S is series resistance and I_{GS} is gate current.

Drain current can be calculated as follows [31]:

$$I_{DS}=I_{SP}\left[\frac{Q_{ch}}{2\eta_q Q_{ch}} - \left(\frac{Q_{ch}}{2\eta_q C_b U_T}\right)\right]^2 \quad (6)$$

Where, I_{SP} is specific current, C_b is barrier capacitance, Q_{ch} is channel charge density, η_q is slope factor, U_T is thermal Voltage.

In this work, by keeping constant drain voltage at 1V and at same time voltage of gate is increased in range from 0V to –4V by 0.1V size of step. The simulated drain current is 0.22A/mm when the drain voltage V_D= 1V. Hence, a 31.81% improvement [29] is achieved using the material AL_2O_3 by considering the electrical properties of the material, as mentioned in Table 1. The Schottky contact between the Gate and AlGaN barrier layer, resulting threshold voltage (V_{TH}) modelling is expressed as [32]

$$V_{TH} = \emptyset_b - \Delta E_C - V_{AlGaN} = \emptyset_b - \Delta E_C - \frac{qN_S d_{AlGaN}}{\varepsilon_0 \varepsilon_{AlGaN}} \quad (7)$$

Where, $\emptyset_b$ is Schottky barrier height, ΔE_C is conduction band difference between GaN and AlGaN, q is charge of electron, N_s is 2DEG density, d_{AlGaN} is AlGaN layer thickness, ε_{AlGaN} is relative dielectric constant. The resulting threshold voltage (V_{TH}) is 3.4V, an 11.76 % [29] improvement in threshold voltage, as shown in Figure. 4

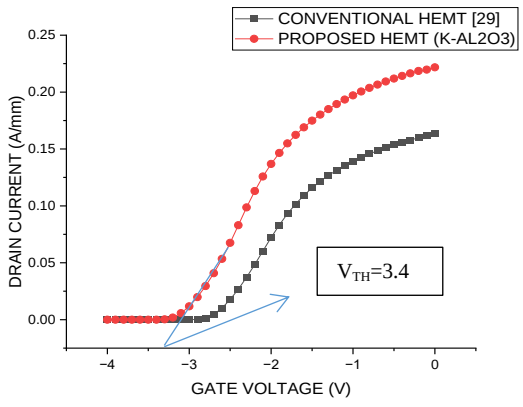

Fig 4. Drain Current versus Gate voltages.

5.2 Gate-Source Capacitance versus Gate Voltage

The importance of gate-source capacitance is to measure the storage capacity of the electric charge. The gate–source capacitance is directly proportional to the controlling gate of the device. Furthermore, some electrical characteristics, such as Noise Figure, linearity, and gain, are improved. Adding the high-K material to the layer positively affects the gate capacitance, which occurs without modifying the physical length of the gate used for compactness applications of the device. The leakage current at the gate electrode was determined by the capacitance between the gate and the source electrodes.

To reduce the leakage current, a larger gate-source capacitance is required. When the voltage increased in the negative direction from 0V to -2V the capacitance remained constant. The obtained maximum capacitance between the gate and source is 3.54×10^{-13}F/mm (2.55×10^{-13}F/mm in [29]), as shown in Fig.5. If we increase the voltage in steps, the capacitance value decreases to 3.03×10^{-13}F/mm (2.18×10^{-13}F/mm [29]). Furthermore, the gate voltage increased in one step from -3V to -4V, and drain voltage V_D= 1V the capacitance value remained unchanged at 8.00×10^{-14}F/mm (5.63×10^{-14}F/mm [29]); therefore, the percentage improvement was 39.99% in comparison with [29]. Ultimately, we can minimize the leakage in gate current as it is inversely proportional to the capacitance between gate and source.

The total amount of charge accumulated on the metal-semiconductor (M-S) is stated bellow:

$$Q_s=\sigma_{surface} = qn_s + \sigma_{substrate}, \quad (8)$$

Where, n_s= 2DEG sheet carrier density.

Hence the capacitance between the gate and source per unit area can be formulated as

$$C_s = \frac{dQ_s}{dv_g} = q\frac{dn_s}{dv_g} + \frac{\sigma_{surface}}{dv_g} \quad (9)$$

Where, v_g denotes gate voltage, q is charge of electron.

Equation (9) can be reduced for the case two cases: case 1: Null impurity charge in substrate and Case 2: Impurity charge density without the gate voltage the function [34].

$$C_s = \frac{dQ_s}{dv_g} = q\frac{dn_s}{dv_g} \quad (10)$$

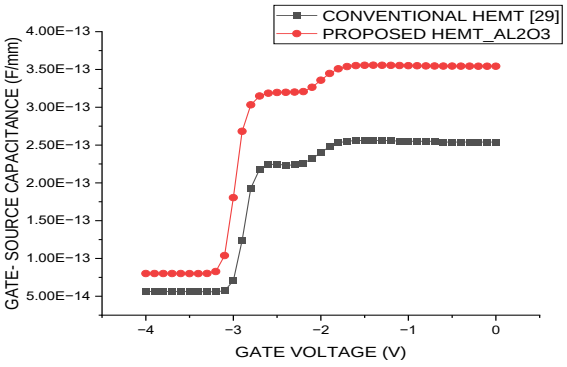

Fig 5. Gate Source Capacitance versus Gate Voltage

5.3 Transcondantance versus Gate Voltage

The performance of the device was identified by determining the value of the transconductance versus voltage across gate, in addition of the gain and device behaviour. Figure.6 shows the sensitivity to variation in the gate voltage propagation efficiency in which the output is controlled by the gate. The conductance was directly proportional to the gain. Therefore, the device exhibited good performance. The gate voltage is changed from 0V to -4V. When voltage is at -2.1V, obtained transconductance (g_m) value is 0.15 S/mm for the material Al_2O_3 [33].

$$\mathbf{g_m} = \frac{\Delta \mathbf{I_D}}{\Delta \mathbf{V_{GS}}} = \left(\frac{\Delta n}{\Delta \mathbf{V_{GS}}}\right)\mathbf{qv} + \left(\frac{\Delta \mathbf{v}}{\Delta \mathbf{V_{GS}}}\right)\mathbf{nq} \qquad (11)$$

Where, q is the charge of an electron, ΔV_{GS} represents change in gate electrode to source electrode voltage, $\Delta I_D$is change in drain current, Δn is noticeable in region of gate for change in ΔV_{GS} , Δn is change in carrier concentration, Δv represents change in carrier velocity.

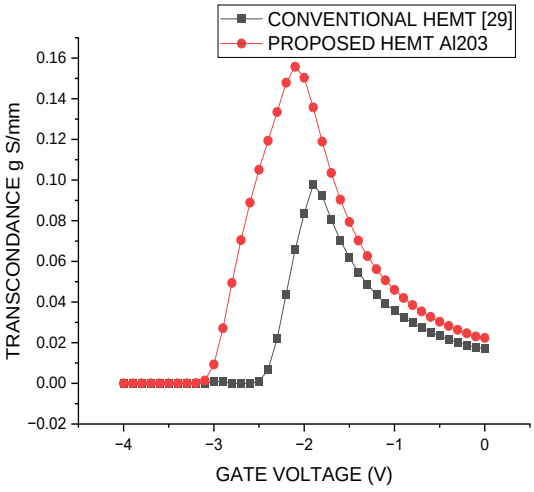

Fig 6. Transcondantance versus gate voltage

4.4 Breakdown Voltage

The breakdown voltage provides the maximum power that can be handled by the device before device damage occurs. Moreover, the use of high-K materials results in the reduction of dielectric breakdown because of electrostatic discharge or hot-carrier injection. The electric field can be decreased by utilizing the high-K material reflected in the increase in the breakdown voltage, with the passivation of Al_2O_3 obtained breakdown voltage (V_{BR}) 350V and drain leakage current

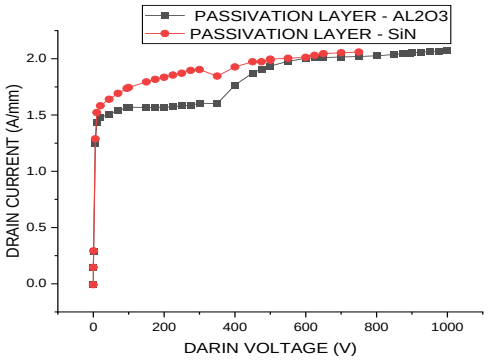

Fig 7. Breakdown Voltage: Drain Current versus Drain Voltage

(I_D) 1.60 A/mm at gate voltage V_G= 3V. Similarly, the passivation of SiN brought breakdown voltage (V_{BR}) 350 and drain leakage current (I_D) 1.84 A/mm at gate voltage V_G= 3V. A 15.00 % improvement in the drain leakage current in the material was observed for Al_2O_3 as shown in Fig. 7.

5.5. Gain versus Frequency

The gain parameter offers the capacity for input signal amplification, regardless of distortion or noise. Such a scenario is vital in the domain of high-frequency applications, where the input signal is too weak, whereas the level of noise is higher. The HEMTs device offers high gain and can amplify a weaker signal to a greater level without introducing distortion or noise.

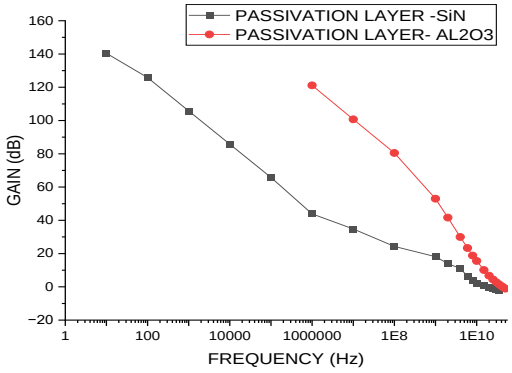

Fig 8. Gain versus Frequency

When the gate voltage V_G= -3V and drain voltage V_D= 1 V, a maximum gain of 121.13dB at a frequency of 1MHz for the material Al_2O_3 was obtained after the simulation. Similarly, by changing the material of the device to SiN, the gain increased to 140dB at a frequency of 10Hz. Gain at frequency 1MHz for both material Al_2O_3 and SiN are

121.13dB and decreased to 43dB respectively as shown in Figure. 8. In terms of percentage improvement is 64.501%.

5.6 Y-Parameter versus Frequency

The relationship between the input voltage, input current, output voltage, and output current is explained by the Y-parameters. The Y parameter helps to optimize HEMT device performance for microwave applications. When the frequency increased from 0Hz to 50GHz the Y_{11} and Y_{22} also increases linearly, as shown in Figure 9. After the Simulation, the obtained maximum value of Y_{11} and Y_{22} are 10.05mho/mm and 12.12mho/mm at gate voltage V_G= -3V and drain voltage V_D= 1V. When we are considering the SiN material at the time of simulation of the device the Y_{11} and Y_{22} are obtained as 8.38mho/mm and 10.73mho/mm. Therefore, we achieved a positive percentage improvement in the proposed device parameters as Y_{11} and Y_{22} of 19.93% and 12.95%, respectively, compared to the conventional device with SiN material. At the same time, we have observed the Y_{12} and Y_{21} parameters as well for material Al_2O_3 such as 2.16 mho/mm and -8.56 mho/mm respectively.

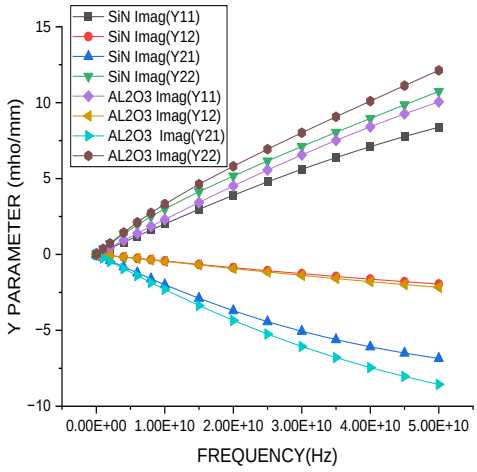

Fig 9. Y-Parameter versus Frequency.

Al_2O_3 material is replaced by the material SiN so obtained maximum values of Y_{12} and Y_{21} are -1.95 mho/mm and -6.85mho/mm respectively. The discussion in terms of percentage improvement with respect to the SiN material is that Y_{12} is improved by 11.24 %, whereas Y_{21} is improved by 24.96 %. All the parameters were calculated at a maximum frequency of 50GHz.

5.7 Conduction Band Energy and Electron Concentration

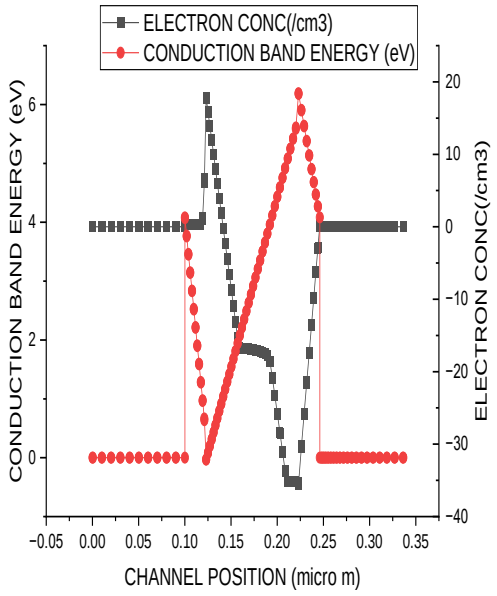

Fig 10. Conduction Band Energy and Electron Concentration versus Channel Position

Based on the conduction band energy diagram, anyone can recognize not only the performance of the HEMT device but also its electron conduction capability. The conduction band energy diagram provides clarity about electron mobility, which shows the movement of free electrons in the device. The conduction-band energy diagram was measured with respect to the channel positions. The conduction band energy level was measured with respect to the channel position, as shown in Fig. 10, in which we observed the conduction band energy versus the channel position from 0µm to 0.35µm. After simulating the proposed device, a zero conduction energy level was observed from the channel position 0 µm to 0.10µm. Furthermore, the energy level increased to 4.06eV, and from the same position, the conduction band energy decreased until the channel position was 0.12µm and again increases. Maximum conduction energy 6.19eV is obtained for the proposed device with material Al_2O_3.In addition to that channel position from 0.22µm to 0.2µm energy level decreases to 4.08eV and remains null afterward. The electron distribution in the HEMT device was determined using an electron-concentration diagram. When an input voltage is applied to the gate electrode, an electric field is created, which accumulates electrons at the HEMT device surface. Therefore, the concentration of electrons was greater in the range adjacent to the gate electrode. The electron concentration was measured with respect to the position of the channels, which helps in finding the noise of the device compatible with the achievement of low-noise performance. Figure 10 also shows the electron concentration. The nature of the electron concentration

changes and is analysed against the channel position from 0µm to 0.3µm. Initially, Electron concentration is 0cm-3 and goes on the increase and reaches 17.82cm^{-3} from 0.1µm to 0.12µm channel position. Furthermore, the amount of concentration of electrons reduced to 35.34cm-^{3} for channel position from 0.12µm to 0.2µm. Electron concentration again increases up to some extent till 4.08cm-3 during the channel position from 0.22µm to 0.24 µm. and becomes null afterward.

5.8 Total Current Density

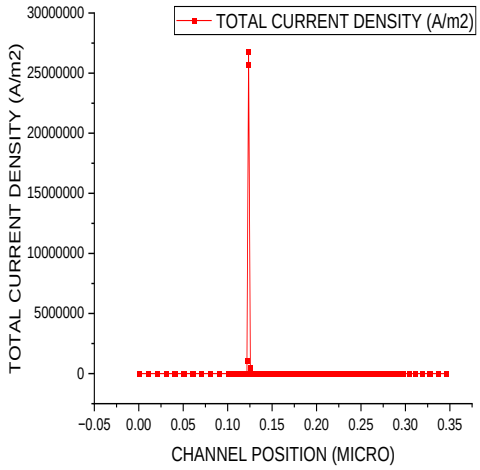

Fig 11. Total Current Density versus channel position

The addition of hole and electron current densities is a useful parameter for obtaining the HEMT device performance. As shown in Figure. 11, the channel position at 0.12µm obtained a total current density of 26794726.6A/mm and the rest of the channel position is 0 A/mm. The multiplication of the electron mobility and electron concentration yields the electron current density. Such parameters offer efficiency and output power of the HEMT device, which are applicable for high-speed and high-power applications such as (Radio Detection and Ranging) RADAR systems and Wireless and Satellite communications.

5.9 Cut-off Frequency versus Gate Voltage

The cut-off frequency is the maximum operating frequency in the range of gigahertz to tens of gigahertz at which the HEMT device can operate effectively. The cut-off frequency can be expressed as follows,

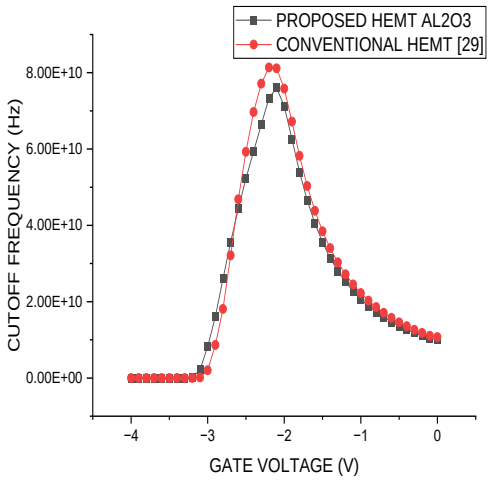

Fig 12. Cut-off Frequency versus Gate Voltage.

$$f_T = \frac{g_m}{2\pi C_{gs}} = \frac{v_{sat}}{2\pi L_g} \quad (12)$$

Where,C_{gs}indicates capacitance between gate and source, v_{sat} indicates saturation carrier velocity and L_g indicates length of gate of the device. From equation (10) it is clearly says that saturation velocity is proportional to the saturation velocity and inversely proportional to the length of the gate of the device [35].

After the simulation of the proposed HEMT device, voltage of gate V_G is varying from 0V to 4V in the negative direction in steps of 1V, and the obtained frequency was analysed. When the gate voltage varies from 0V to -1.9V, the frequencies increase exponentially and do not change for the Al_2O_3 and SiN passivation materials, as shown in Figure.12. If the gate voltage is varying from -1.9V to -2.1V there is a slight change in frequency. At gate voltage -2.1V Cut-off frequencies obtained is 76.0GHz for the passivation Al_2O_3 and for passivation material SiN 81.4GHz is obtained Cut-off frequency. It was observed that the cut-off frequency decreased by 9.63%. The obtained frequency 35.6 GHz is the same at gate voltage -2.7V for both passivation materials. When the gate voltage is -3.1V frequency is 21.6GHz and becomes zero when the gate voltage increases from -3.1V to -4V for the case of Al_2O_3. The device with SiN material emits a frequency of 20.0GHz at gate voltage -3V and becomes null when gate voltage increases from -3V to -4V.

Table 4. Result analysis of proposed device

Electrical Parameters ↓	**Proposed HEMT with Al_2O_3**	**[29]**	**Percentage Improvement (%)**
Darin Current (A/Mm)	0.22	0.15	**31.81 [29] (INC-REMENT)**
Capacitance between Gate and Source ($C_{gs\ Max}$)(F/Mm)	3.54×10^{-13} F/mm	2.54×10^{-13} F/mm	**39.33 [29] (DECRE-MENT)**
Tranconductance (G_m)(S/mm)	0.15	0.09	**25 [29] (INCRE-MENT)**
Breakdown Voltage (V_{BR})(V)	350 V at I_D=1.84 (A/mm)	-	**EXTRA RESULT DROWN (ERD)**
Maximum Drain Voltage(V_{DMax}) (V)	1000	-	**ERD**
Gain (dB)	121.13 at 1 MHz	-	**ERD**
Y Parameters At 50 GHz Y_{11}	10.05	-	**ERD**
Y_{12}	-2.16		
Y_{21}	-8.56		
Y_{22}	12.12		
Cutoff Frequency (Hz)	76.0 GHz 7.60×10^{10} Hz at -2.1 V	81.4 GHz 8.14×10^{10} Hz at -2.1 V	**9.63 (DECRE-MENT)**

6. Conclusion

The performance improvement of AlGaN/GaN high-electron-mobility transistors (HEMTs) using the high-K technique presents a promising avenue for enhancing the efficiency and functionality of electronic devices. The integration of high-K dielectric materials into the gate stack of HEMTs offers several advantages, including reduced gate leakage current, improved gate control, and enhanced breakdown voltage. The incorporation of high-K materials such as HfO_2 or Al_2O_3 allows for a higher capacitance at the gate, enabling better gate modulation and increased transconductance. Obtained electrical parameters are Darin Current is 0.22A/mm with 31.81% decrement, Gate-Source Capacitance ($C_{gs\ Max}$) is 3.54×10^{-13}F/mm with 39.33 % decrement, Tranconductance (G_m) 0.15S/mm, Breakdown Voltage (V_{BR}) 350V at I_D-=1.84 (A/mm), Maximum Drain Voltage (V_{DMax}) is 1000V, Gain is 121.13dB at 1MHz, Cut-off Frequency is 76.0 GHz at -2.1V with decrement of 9.63% which needs to be improved in future. Overall, the performance enhancement achieved through the

incorporation of high-K techniques in AlGaN/GaN HEMTs holds significant potential for advancing the field of electronics, enabling the development of more efficient and reliable devices for a wide range of applications such radio-frequency devices, and high-speed digital circuits.

References:

[1]. Chen, M.J., Wang, X.P., Hu, C., Han, G., Tan, C.H. and Yeo, Y.C.,(2004). High-k gate dielectrics: Current status and materials properties considerations. *Journal of Applied Physics, 96(4)*, pp.2019-2034.

[2]. Park, M., Lee, S., and Park, K., (2006). High-k gate dielectrics for future metal–oxide–semiconductor field-effect transistors. *Journal of Applied Physics, 99(8),* p.081301.

[3]. Houssa, M., Pourtois, G., Afanas'ev, V.V. and Stesmans, A., (2008). High-k materials for MOS gate dielectric layers. *Materials Science and Engineering: R: Reports, 64(1-3),* pp.1-53.

[4]. Osten, H.J. and von Schwerin, A.,(2010). High-k materials for nanoelectronics: Current status and materials properties considerations. *Journal of Applied Physics, 107(2),* p.021101.

[5]. Robertson, J., (2012). High dielectric constant gate oxides for metal oxide Si transistors. *Reports on Progress in Physics, 75(3),* p.034501.

[6]. Zhu, M., Li, M.F., Seng, H.L., Tan, C.H. and Lo, G.Q., (2013). High-k gate dielectric materials for advanced CMOS devices. *Progress in Materials Science, 58(6),* pp.825-873.

[7]. Lee, J.C., Cui, Y., Duan, C., Guo, H., Wang, K.L., Palacios, T., Chen, Y.C. and Kim, T.W., (2015). Advanced high-k dielectric materials for future gate stack of advanced CMOS and beyond. *ECS Journal of Solid State Science and Technology, 4(4),* pp.Q3090-Q3101.

[8]. Kwo, J., Hong, M., Chu, J., and Chen, M.J., (2017). High-K Gate Dielectrics for Emerging Devices: Materials, Physics, and Engineering. *Annual Review of Materials Research, 47,* pp. 49-85.

[9]. Qi, X., Huang, R. and Gan, F., (2019). High-k dielectric materials for advanced metal–oxide–semiconductor field-effect transistor applications. *Journal of Materials Science: Materials in Electronics*, 30(9), pp.7998-8017.

[10]. Touati Zine-eddine, Hamaizia Zahra, Messai Zitouni, Design and analysis of 10 nm T-gate enhancement-mode MOS-HEMT for high power microwave applications *Journal of Science: Advanced Materials and Devices.*

[11]. L. Xu, N. Gao, Z. Zhang, and L.-M. Peng, , (2018) Lowering interface state density in carbon nanotube thin film transistors through using stacked Y_2O_3/HfO_2 gate dielectric *Appl. Phys. Lett., vol. 113, no. 8, pp*. 083105.

[12]. C. H. Lee, C. Lu, T. Tabata, W. F. Zhang, T. Nishimura, K. Nagashio, and A. Toriumi (2013). Oxygen Potential Engineering of Interfacial Layer for Deep Sub-nm EOT High-k Gate Stacks on Ge," *IEEE International Electron Devices Meeting(IEDM), pp*. 2.5.1-2.5.4.

[13]. S. H. Kim, D. M. Geum, M. S. Park, and W. J. Choi (2015). In0.53Ga0.47As-on-Insulator Metal–Oxide–Semiconductor Field-Effect Transistors Utilizing Y2O3 Buried Oxide," *IEEE Electron Device Lett.*, vol. 36, no. 5, pp.451-453.

[14]. H. Hanawa, H. Onodera, A. Nakajima, and K. Horio, (2014). Numerical analysis of breakdown voltage enhancement in AlGaN/GaN HEMTs with a high-k passivation layer," *IEEE Transactions on Electron Devices*, vol. 61, no. 3, pp. 769-775.

[15]. S. Yang, Z. Tang, K.-Y. Wong, Y.-S. Lin, C. Liu, Y. Lu, S. Huang, and K. J. Chen (2013) High-quality interface in Al2O3/GaN/AlGaN/GaN MIS structures with in situ pre-gate plasma nitridation. *IEEE Electron Device Letters, vol. 34, no. 12*, pp. 1497-1499.

[16]. R. Stoklas, D. Gregušová, M. Blaho, K. Fröhlich, J. Novák, M. Matys, Z. Yatabe, P. Kordoš, and T. Hashizume, (2017) Influence of oxygen-plasma treatment on AlGaN/GaN metal-oxide-semiconductor heterostructure field-effect transistors with HfO_2 by atomic layer deposition: leakage current and density of states reduction. *Semiconductor Science and Technology, vol. 32, no. 4*, pp. 045018, 2017.

[17]. H. Jiang, C. Liu, K. W. Ng, C. W. Tang, and K. M. Lau, (2018) High-performance AlGaN/GaN/Si power MOSHEMTs with ZrO2 gate dielectric. *IEEE Transactions on Electron Devices, vol. 65, no*. 12, pp. 5337-5342, 2018.

[18]. C.-S. Lee, W.-C. Hsu, B.-J. Chiang, H.-Y. Liu, and H.-Y. Lee, (2017). Comparative studies on AlGaN/GaN/Si MOS-HFETs with Al2O3/TiO2 stacked dielectrics by using an ultrasonic spray pyrolysis deposition technique .*Semiconductor Science and Technology, vol. 32, no. 5, pp*. 055012, 2017.

[19]. K. Nishiguchi, J. Ohira, S. Kaneki, S. Toiya, and T. Hashizume (2016). Controllability improvement of Al2O3-gate structure for GaN transistors" *Compound Semiconductor Week 2016* 978-1-5090-1964-9/16/$31.00 ©2016 IEEE.

[20]. Bo-Yi Chou, Han-Yin Liu, Wei-Chou Hsu, Ching-Sung Lee1, Yu-Sheng Wu, and En-Ping Yao. "Electrical and Reliability Performances of Stacked HfO2/Al2O3 MOS-HEMTs", 978-1-4799-3197-2/14/$31.00 ©2014 IEEE.

[21]. Kenya Nishiguchi *et al (* 2017). Current linearity and operation stability in Al_2O_3- gate AlGaN/GaN MOS high electron mobility. *Japanese Journal of Applied Physics transistorsJpn. J. Appl. Phys.* 56 101001.

[22]. Yuji Ando1, Shota Kaneki1, and Tamotsu Hashizume. (2019). Improved operation stability of Al_2O_3/AlGaN/GaN MOS high-electron-mobility transistors grown on GaN substrates. *Applied Physics Express 12*, 024002.

[23]. J. Buckley, M. Bocquet, G. Molas, M. Gely, P. Brianceau, N. Rochat, E.Martinez, F.Martin, H. Grampeix, JP. Colonna, A.Toffoli, V. Vidal, C. Leroux, G. Ghibaudo, G. Pananakakis, C. Bongiorno, D. Corso, S. Lombardo, B. DeSalvo, S.Deleonibus,In-depth Investigation of Hf-based High-k Dielectrics as Storage Layer of Charge-Trap NVMs, CNR-IMM, Stradale Primosole 95121 Catania, Italy.

[24]. G. Ribes, J. Mitard, M. Denais, S. Bruyere, F. Monsieur, C. Parthasarathy, E. Vincent, and G. Ghibaudo (2015) Review on High-k Dielectrics Reliability Issues *IEEE TRANSACTIONS ON DEVICE AND MATERIALS RELIABILITY*, VOL. 5, NO. 1.

[25]. Yutao Cai, Yang Wang, Miao Cui, Wen Liu, Huiqing Wen, Cezhou Zhao Paul R. Chalker. Effect of High-k Passivation Layer on Electrical Properties of GaN Metal-Insulator-Semiconductor Device. *University of Liverpool, Liverpool, L69 3GJ, UK.*

[26]. O Ambacher, J Majewski, C Miskys, A Link, M Hermann, M Eickhoff, M Stutzmann, F Bernardini, V, V Tilak, B Schaff and L F Eastman(2002), Pyroelectric properties of Al(In)GaN/GaN heteroand quantum well structures, *J. Phys.: Condense. Matter*, *14 :3399–3434. https://doi.org/10.1088/0953- 8984/14/13/302*.

[27]. Santa Clara (2016) ,Device Simulation Software *SILVACO Int. ATLAS User's Manual;* , CA, USA, Available online: https://www.silvaco.com.

[28]. M. Farahmand; C. Garetto; E. Bellotti; K.F. Brennan; M. Goano; E. Ghillino; G. Ghione; J.D. Albrecht; P.P. Ruden (2001) Monte Carlo simulation of electron transport in the III-nitride wurtzite phase materials system: binaries and ternaries, *IEEE Transactions on Electron Devices*, vol. 48:535-542. https://doi.org/10.1109/16.906448

[29]. Aboo Bakar Khan and M. J. Siddiqui (2019) Impact of Back Barrier with Back Gate on Device Performance of AlGaN/GaN DG-HEMT *Journal of Nanoelectronics and Optoelectronics Vol. 14, pp. 1–6.*

[30]. A. Soltani, , M. Rousseau, J.-C. Gerbedoen, M. Mattalah, P. L. Bonanno, A. Telia, N. Bourzgui, G. Patriarche, A.Ougazzaden, and A. BenMoussa (2014); High performance TiN gate contact on AlGaN/GaN transistor using a mechanically strain induced P-doping *Appl. Phys. Lett. American Institute of Physics* 104, 233506 doi: 10.1063/1.4882415

[31]. Farzan Jazaeri and Jean-Michel Sallese (2019)Charge-Based EPFL HEMT Model, *IEEE TRANSACTIONS ON ELECTRON DEVICES*, VOL. 66, NO. 3.

[32]. Hyeon-Tak Kwak 1, Seung-Bo Chang 1, Hyun-Jung Kim 1, Kyu-Won Jang 1, Hyung Sup Yoon 2, Sang-Heung Lee 2, Jong-Won Lim 2 and Hyun-Seok Kim 1 Operational Improvement of AlGaN/GaN High Electron Mobility Transistor by an Inner Field-Plate Structure

[33]. Sushanta Bordoloi, Ashok Ray, D Gaurav Trivedi, (2021) Introspection Into Reliability Aspects in AlGaN/GaN HEMTs With Gate Geometry Modification *Published in: IEEE Access (Volume: 9)* Page(s): 99828 – 99841 Electronic ISSN: 2169-3536 INSPEC Accession Number: 21074305 DOI: 10.1109/ACCESS.2021.3096988

[34]. Wang Xin-Hua,Zhao Miao, Liu Xin-Yu,Pu Yan,Zheng Ying-Kui, and Wei Ke. (2010) The physical process analysis of the capacitance voltage characteristics of AlGaN/AlN/GaN high electron mobility transistors. Chin. Phys. B Vol. 19, No. 9 097302.

[35]. Fu, W., Xu, Y., Yan, B., Zhang, B. and Xu, R.,(2013) Numerical simulation of local doped barrier layer AlGaN/GaN HEMTs. Superlattices and Microstructures, 60, pp.443–452.

[36]. P, R. H. ., B, S. D. ., M, D. K. ., Sooda, K. ., & B, K. R. . (2023). Transfer Learning based Automated Essay Summarization. International Journal on Recent and Innovation Trends in Computing and Communication, 11(1), 20–25. https://doi.org/10.17762/ijritcc.v11i1.5983

[37]. Smith, J., Jones, D., Martinez, J., Perez, A., & Silva, D. Enhancing Engineering Education through Machine Learning: A Case Study. Kuwait Journal of Machine Learning, 1(1). Retrieved from http://kuwaitjournals.com/index.php/kjml/article/view/86